

The Silicon Vertex Detector of the Belle II experiment

2 **A.B. Kaliyar**,^{a,*} **K. Adamczyk**,^b **L. Aggarwal**,^c **H. Aihara**,^d **T. Aziz**,^e **S. Bacher**,^b
 3 **S. Bahinipati**,^f **G. Batignani**,^{g,h} **J. Baudot**,ⁱ **P. K. Behera**,^j **S. Bettarini**,^{g,h} **T. Bilka**,^k
 4 **A. Bozek**,^b **F. Buchsteiner**,^a **G. Casarosa**,^{g,h} **L. Corona**,^h **S. B. Das**,^l **G. Dujany**,ⁱ
 5 **C. Finck**,ⁱ **F. Forti**,^{g,h} **M. Friedl**,^a **A. Gabrielli**,^{m,n} **B. Gobbo**,ⁿ **S. Halder**,^e **K. Hara**,^{o,p}
 6 **S. Hazra**,^e **T. Higuchi**,^q **C. Irmeler**,^a **A. Ishikawa**,^{o,p} **Y. Jin**,ⁿ **M. Kaleta**,^b **J. Kandra**,^k
 7 **K. H. Kang**,^q **P. Kodyš**,^k **T. Kohriki**,^o **R. Kumar**,^r **K. Lalwani**,^l **K. Lautenbach**,^t
 8 **R. Leboucher**,^t **S. C. Lee**,^s **J. Libby**,^j **L. Martel**,ⁱ **L. Massaccesi**,^{g,h} **G. B. Mohanty**,^e
 9 **S. Mondal**,^{g,h} **K. R. Nakamura**,^{o,p} **Z. Natkaniec**,^b **Y. Onuki**,^d **F. Otani**,^q
 10 **A. Paladino**,^{A, g,h} **E. Paoloni**,^{g,h} **H. Park**,^s **L. Polat**,^t **K. K. Rao**,^e **I. Ripp-Baudot**,ⁱ
 11 **G. Rizzo**,^{g,h} **Y. Sato**,^o **C. Schwanda**,^a **J. Serrano**,^t **T. Shimasaki**,^q **J. Suzuki**,^o
 12 **S. Tanaka**,^{o,p} **H. Tanigawa**,^d **F. Tenchini**,^{g,h} **R. Thalmeier**,^a **R. Tiwary**,^e
 13 **T. Tsuboyama**,^o **Y. Uematsu**,^d **L. Vitale**,^{m,n} **Z. Wang**,^d **J. Webb**,^u **O. Werbycka**,ⁿ
 14 **J. Wiechczynski**,^b **H. Yin**^a and **L. Zani**^{B,t}

15 ^a*Institute of High Energy Physics, Austrian Academy of Sciences, 1050 Vienna, Austria*

16 ^b*H. Niewodniczanski Institute of Nuclear Physics, Krakow 31-342, Poland*

17 ^c*Punjab University, Chandigarh 160014, India*

18 ^d*Department of Physics, University of Tokyo, Tokyo 113-0033, Japan*

19 ^e*Tata Institute of Fundamental Research, Mumbai 400005, India*

20 ^f*Indian Institute of Technology Bhubaneswar, Bhubaneswar 752050, India*

21 ^g*Dipartimento di Fisica, Università di Pisa, I-56127 Pisa, Italy, ^Apresently at INFN Sezione di Bologna,*
 22 *I-40127 Bologna, Italy*

23 ^h*INFN Sezione di Pisa, I-56127 Pisa, Italy*

24 ⁱ*IPHC, UMR 7178, Université de Strasbourg, CNRS, 67037 Strasbourg, France*

25 ^j*Indian Institute of Technology Madras, Chennai 600036, India*

26 ^k*Faculty of Mathematics and Physics, Charles University, 121 16 Prague, Czech Republic*

27 ^l*Malaviya National Institute of Technology Jaipur, Jaipur 302017, India*

28 ^m*Dipartimento di Fisica, Università di Trieste, I-34127 Trieste, Italy*

29 ⁿ*INFN Sezione di Trieste, I-34127 Trieste, Italy*

30 ^o*High Energy Accelerator Research Organization (KEK), Tsukuba 305-0801, Japan*

31 ^p*The Graduate University for Advanced Studies (SOKENDAI), Hayama 240-0193, Japan*

32 ^q*Kavli Institute for the Physics and Mathematics of the Universe, University of Tokyo, Kashiwa 277-8583,*
 33 *Japan*

34 ^r*Punjab Agricultural University, Ludhiana 141004, India*

35 ^s*Department of Physics, Kyungpook National University, Daegu 41566, Korea*

*Speaker

36 ¹*Aix Marseille Université , CNRS/IN2P3, CPPM, 13288 Marseille, France, ^Bpresently at INFN Sezione di*
37 *Roma Tre, I-00185 Roma, Italy*

38 ⁴*School of Physics, University of Melbourne, Melbourne, Victoria 3010, Australia*

39 *E-mail: abdulbasith.kaliyar@oeaw.ac.at*

The Belle II silicon vertex detector (SVD) is a four-layer double-sided silicon strip detector installed within the Belle II detector located at KEK, Japan. SVD has been operating smoothly and reliably since the start of data taking in March 2019. The data quality and radiation damage effects have been constantly monitored. In this article, we report the operational experience of SVD, reconstruction performance and effects of beam background and radiation damage. We also report some of the recent efforts to improve the software robustness targeting the high luminosity scenario and hardware activities performed during the first long shutdown of Belle II experiment.

1. Introduction

The Belle II experiment [1] aims to make precise measurements of weak interaction parameters, study exotic hadrons, and search for new physics beyond the Standard Model of particle physics. The experiment is currently underway at the SuperKEKB accelerator research center located in Tsukuba, Japan. The SuperKEKB [2] is an asymmetric energy e^- (7 GeV) e^+ (4 GeV) collider operates near the $\Upsilon(4S)$ resonance (10.58 GeV). The instantaneous peak luminosity achieved so far is $4.7 \times 10^{34} \text{cm}^{-2}\text{s}^{-1}$, which is the world record and more than twice that of KEKB accelerator, the predecessor of SuperKEKB. The ultimate target is to reach a peak luminosity of $6 \times 10^{35} \text{cm}^{-2}\text{s}^{-1}$. The Belle II detector is positioned around the interaction point of the SuperKEKB and has so far collected 430fb^{-1} of data. The eventual goal is to collect 50ab^{-1} of data in the next decade.

The Vertex Detector (VXD) is the innermost subdetector in the Belle II detector system located closest to the interaction point. Comprising six layers, it includes two inner layers of pixel detector (PXD) [3], based on depleted field effect transistor (DEPFET) sensors, and four outer layers of silicon strip detector, known as the silicon vertex detector (SVD) [4]. The SVD is crucial for extrapolating the measured tracks to the PXD and point at a region-of-interest that helps to significantly reduce the amount of data recorded by PXD. Besides, SVD also performs standalone tracking of low-momentum particles, vertex detection of K_S^0 and Λ particles, and contributes to the charged-particle identification by providing energy-loss information (dE/dx).

In July 2022, Belle II temporally paused operation for the first long shutdown (LS1) to allow the maintenance work of the accelerator and improvements in detector. VXD was re-installed during this time with a new complete PXD and the same SVD. In this report we present a detailed description of the SVD, its performance until July 2022, effects of radiation damage and the software improvements towards high luminosity scenario and the main challenges and results of the VXD re-installation during LS1.

2. Belle II Silicon Vertex Detector

The Belle II SVD is composed of four layers of Double-Sided Silicon Strip Detector (DSSD), namely layer 3, 4, 5 and 6, placed at a radii of 39, 80, 104, and 135 mm, respectively, from the beam pipe. The material budget is about 0.7% of a radiation length per layer. In total, there are 172 sensors with a sensor area of 1.2m^2 and 224 thousand readout strips. There are three types of DSSDs: “small” rectangular sensors in layer 3, “large” rectangular sensors in the barrel region of layers 4, 5, and 6, and “trapezoidal” sensors in the forward region of layers 4, 5, and 6, that are slanted. These sensors are made from an N-type bulk 6-inch wafer with a thickness of about $300 \mu\text{m}$. To provide two-dimensional spacial information, P side strips of the sensors are placed parallel to the beam axis while the N side strips are placed transverse to the beam axis. The details of the DSSDs are summarized in Table 1. The readout strips are AC coupled and there is one intermediate floating strip between two readout implants. The full depletion voltage ranges from 20 – 60 V, and the operating voltage is 100 V. The radiation hardness of SVD sensors is about 6 Mrad.

The front-end readout ASIC used in SVD is APV25 [5] chips, with 128 input channels. The signals from the strips are collected by APV25 chips and provide analog readout. APV25 chip has

Table 1: Details of the three types of DSSDs used in the SVD.

	Small rectangular	Large rectangular	Trapezoidal
Sensor active area (mm ²)	122.90 × 38.55	122.90 × 57.52	122.76 × (38.42 – 57.59)
Number of P-strips	768	768	768
P-strip readout pitch (μm)	50	75	50 – 75
Number of n-strips	768	512	512
N-strip readout pitch (μm)	160	240	240
Thickness (μm)	320	320	300
Manufacturer	Hamamatsu	Hamamatsu	Micron

81 a fast 50 ns shaping time and a radiation hardness up to 100 Mrad. By default, the chip operates in
 82 multi-peak mode at a clock frequency of 31.8 MHz which is 1/8 of the SuperKEKB bunch-crossing
 83 frequency. Six consecutive samples are read out upon the arrival of a global hardware trigger to
 84 reconstruct the signal pulses. To save the data transmission bandwidth at the high luminosity runs,
 85 a 3/6-mixed operation mode is also developed, where three or six samples are acquired depending
 86 on the timing precision of the hardware trigger. The 3/6-mixed mode operation mode has been
 87 tested and is ready to use in the future.

88 3. Operation and performance

89 The SVD has been operating smoothly and reliably since its installation in 2019. The total
 90 fraction of masked strips due to defects is less than 1% and only one out of 1748 APV25 chip was
 91 temporarily disabled. Temperature and calibration constants are evolving in the expected ranges
 92 due to radiation damage. The hit efficiency exceeds above 99% for all the sensors. Figure 1 shows
 93 example distributions of cluster charge and cluster signal-to-noise ratio (SNR) measured in 2022
 94 and 2020. The signal cluster charge is normalized to the track path length in the silicon to correct
 95 for the track’s incidence angle. The normalized cluster charge is found to be in good agreement
 96 with expectations and similar in all sensors. The charge matches with the expected minimum
 97 ionizing particle (MIP) value of approximately 24000 e^- within 15%, which is the uncertainty in
 98 the absolute APV25 gain calibration. The cluster SNR is defined as the total cluster charge divided
 99 by the quadratic sum of the noise values from each strip in the cluster. A small decrease of cluster
 100 SNR is observed in 2022 data, due to increased noise from radiation damage ($\sim 20\% - 30\%$).
 101 In general, very good SNR is measured across all 172 DSSD sensors, with most probable value
 102 typically falling within the range of 13 to 30, varying based on sensor side and position.

103 The cluster position resolution is crucial in vertexing and track reconstruction performance.
 104 The position resolution of the SVD is estimated from the residual of cluster positions with respect
 105 to unbiased track extrapolation after subtracting the effect of the track extrapolation uncertainty [6].
 106 Studies using dimuon ($e^+e^- \rightarrow \mu^+\mu^-$) events shows a resolution of 7 – 12 μm for the P side and
 107 15 – 25 μm for the N side. These are in fair agreement with expectations from the sensor pitch.
 108 Good stability of position resolution over the time is also confirmed by comparing measurements
 109 from 2022 to 2020.

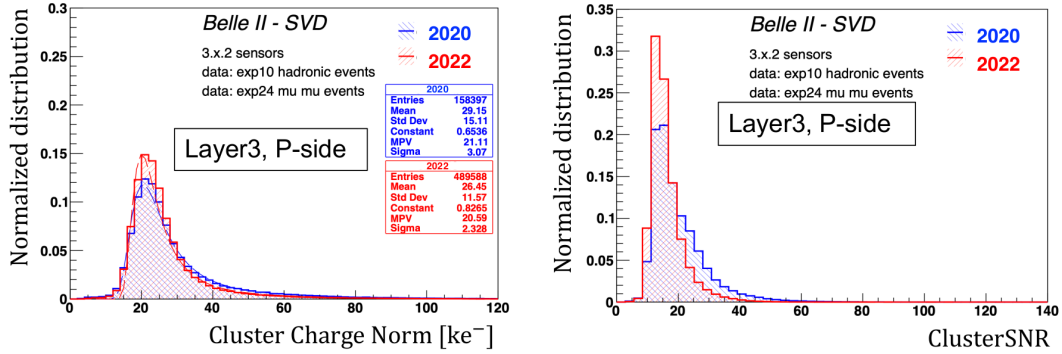


Figure 1: The signal cluster charge (left) and the cluster SNR (right) in P strips for one of Layer 3 sensors.

110 The SVD also offers an excellent hit time resolution. It is measured from the residuals of
 111 the hit time with respect to the time of the e^+e^- collision (EventT0) provided by the central drift
 112 chamber (CDC) of the Belle II detector. The measured hit time resolution is 2.9 ns (2.4 ns) for
 113 the P (N) side. The hit time information is also used to remove the machine related background,
 114 which is typically unassociated with the e^+e^- collisions. These off time hit background enters the
 115 triggered data acquisition window and increase the strip occupancy. Background occupancy above
 116 a certain threshold can cause tracking performance degradation. Time difference between the P and
 117 N side clusters can also be used to suppress the wrong combination of P and N side clusters when
 118 there are more than one particle crossing one piece of sensor. By requiring the cluster time within
 119 50 ns of the event time and time difference between P and N side cluster within 20 ns, 50% off-time
 120 background hits can be rejected while keeping 99% tracking efficiency. This allows us to set the hit
 121 occupancy limit at layer 3 to 4.7% without tracking performance deterioration.

122 Two new algorithms are currently being developed that exploit the SVD time information
 123 to further relax the hit-occupancy limit and enhance the offline software robustness in the high-
 124 background environment. One method involves the selection of track-time, which is computed by
 125 combining the hit-time of SVD clusters associated with a track. This reduces the fake-track rate,
 126 thus relaxing the hit-occupancy limit. The second algorithm involves grouping SVD clusters using
 127 the hit-time information. The cluster time distribution has clear grouping structure since clusters
 128 from different bunches are collected within the acquisition time window of the triggered event.
 129 Signal clusters are located in a group around the event-time, $T = 0$, while other background hits
 130 form other groups, which are caused by other beam-bunches. Since many background hits are
 131 within the 50 ns range, it cannot be eliminated completely with a hit-time selection alone. The
 132 cluster grouping method allows event-by-event classification and further background elimination.
 133 The addition of these two new algorithms allow us to set the hit-occupancy limit at around 6%.
 134 Further software improvement and optimization are currently ongoing before incorporating these
 135 features to the actual data processing.

136 4. Beam Background and Radiation Effects

137 In this section we discuss the effects of radiation damage on the SVD sensors during its
138 operation. The beam-induced background increases the hit occupancy and causes radiation damage
139 to the sensors. The radiation damage affects the strip noise, leakage current, and full depletion
140 voltage of sensors and it is constantly monitored during the operation. Current average hit
141 occupancy on layer 3 sensors is less than 0.5% and well under control. Radiation dose in the SVD
142 is estimated based on the data from diamond sensors that are mounted on the beam pipe and the
143 bellows pipes outside of the VXD. The total integrated radiation dose on Layer-3 sensors is 70 krad,
144 which corresponds to an equivalent 1 – MeV neutron fluence of $1.6 \times 10^{11} n_{\text{eq}}/\text{cm}^2$, assuming the
145 ratio of a neutron fluence to a radiation dose of $2.3 \times 10^9 n_{\text{eq}}/\text{cm}^2/\text{krad}$ based on MC simulation.

146 The strip noise, which is dominated by the inter-strip capacitance, during the operation increased
147 about 20% (30%) for N-side (P-side), which is expected to be saturated. The leakage current is
148 gradually increasing and, in general, its value shows a linear dependence on the accumulated dose,
149 as expected from NIEL model. So far, this increase has negligible contribution to the noise because
150 of small leakage current and short APV25 shaping time. However, after 6 Mrad the leakage current
151 contribution to noise might become significant and reduces the SNR in the layer 3 below 10. So far
152 no changes in full depletion voltage are observed in the operating sensors.

153 Further studies have been carried out with several irradiation campaigns to better evaluate the
154 radiation tolerance of SVD sensors even after bulk type inversion. In July 2022, a new irradiation
155 campaign of SVD sensors was performed with 90 MeV e^- beam at ELPH, Tohoku University, with
156 a radiation dose up to 10 Mrad (corresponding to $3 \times 10^{13} n_{\text{eq}}/\text{cm}^2$ of neutron fluence). The type
157 inversion of the sensor bulk is confirmed after 2 Mrad of radiation. The tests confirm that the SVD
158 sensor works well even after the bulk type inversion which is expected from previous experience of
159 silicon detectors of similar type. These results provide a large safety margin for SVD even after 10
160 years of operation at target luminosity.

161 5. VXD reinstallation during Long Shutdown 1

162 In July 2022, Belle II paused its operation for the first long shutdown to allow the maintenance
163 work of the accelerator and implement upgrades to the detector. A brand new pixel detector (PXD2)
164 with fully installed second layer was installed in the VXD volume along with the current SVD.
165 Very intense hardware activities were carried out involving the SVD crew during the de-installation
166 and re-installation of VXD. On 10 May, 2023, the VXD was safely extracted from the Belle II
167 detector, followed by dismantling two SVD half-shells from the old PXD and mounting them on
168 PXD2. All these delicate operations involved several steps with extensive testing of the detector
169 and the environmental monitoring system, to ensure the healthiness of the system after each step.
170 The healthiness of all SVD sensors were confirmed during the commissioning of the new VXD
171 in the clean room. On 28 July, 2023, the new VXD was successfully reinstalled into the Belle II
172 detector. Additional tests including cosmic ray runs were performed before the start of the actual
173 beam operations. After LS1, Belle II officially restarted data taking in January 2024, and so far
174 SVD is performing smoothly as before.

175 **6. Conclusion**

176 The Belle SVD has been taking high-quality data since March 2019. Operation is stable and
177 reliable with excellent detector performance. Effects from radiation damage are observed at the
178 expected level, however their contribution does not cause any degradation to the SVD tracking
179 performance so far. During the first long shutdown, a new VXD was successfully re-installed into
180 the Belle II detector incorporating the full PXD2 together with the existing SVD.

181 Background extrapolation to the target luminosity as well as the results of irradiation campaign
182 show that the SVD is safe even after 10-years operation. However, the high background environment
183 in the future may deteriorate tracking performance of the SVD as indicated by the simulation. To
184 enhance the robustness against high background, as well as matching the possible new interaction
185 region, technology assessment is ongoing for a possible VXD upgrade during the second long
186 shutdown of the Belle II operation [7–9].

187 **7. Acknowledgements**

188 This project has received funding from the European Union’s Horizon 2020 research and
189 innovation programme under the Marie Skłodowska-Curie grant agreements No 644294, 822070
190 and 101026516 and ERC grant agreement No 819127. This work is supported by MEXT, WPI
191 and JSPS (Japan); ARC (Australia); BMBWF (Austria); MSMT (Czechia); CNRS/IN2P3 (France);
192 AIDA-2020 (Germany); DAE and DST (India); INFN (Italy); NRF and RSRI (Korea); and MNiSW
193 (Poland).

194 **References**

- 195 [1] T. Abe, *et al.*, Belle II Technical Design Report [[arXiv:1011.0352](https://arxiv.org/abs/1011.0352)].
- 196 [2] Y. Ohnishi, *et al.*, Prog. Theor. Exp. Phys. **2013**, 03A011 (2013).
- 197 [3] B. Wang, *et al.*, Nucl. Instrum. Meth. A **1032**, 166631 (2022).
- 198 [4] K. Adamczyk, *et al.*, JINST **17**, P11042 (2022).
- 199 [5] M. J. French, *et al.*, Nucl. Instrum. Meth. A **466**, 359 (2001).
- 200 [6] R. Leboucher, *et al.*, Nucl. Instrum. Meth. A **1033**, 166746 (2022).
- 201 [7] Belle II Collaboration, Snowmass Whitepaper: The Belle II Detector Up- grade Program,
202 [[arXiv:2203.11349](https://arxiv.org/abs/2203.11349) (2022)].
- 203 [8] M. Babeluk, *et al.*, Nucl. Instrum. Meth. A **1048** 168015 (2023).
- 204 [9] A. Ishikawa, *et al.*, Nucl. Instrum. Meth. A **978**, 164404 (2020).